Astronomy with Millimeter and Submillimeter Wave Interferometry
ASP Conference Series, Vol. 59, 1994
M. Ishiguro and Wm. J. Welch (eds.)

INTERFEROMETRIC OBSERVATIONS OF HCO^+ AND HCN IN THE NUCLEAR REGION OF IC 342 AND MAFFEI 2.

Nguyen-Rieu[1], F. Viallefond[1],
F. Combes[1], J.M. Jackson[2], J. Lequeux[1], S. Radford[3] and Truong-Bach[1]

1)Observatoire de Paris-Meudon, F-92195 Meudon Principal Cedex, France
2)Boston University, Dept. of Astronomy, 725 Commonwealth Ave. MA 02215, USA
3)Institut de Radio Astrononmie Millimetrique, F-38406, St. Martin d'Heres, France

ABSTRACT The IRAM interferometer has been used to image the distribution and kinematics of the HCO^+ line in the nuclear region of IC 342 and of the HCN line in the nuclear region of Maffei2. Both regions were also imaged in the continuum at 3mm. These observations are compared with observations of HCN in IC 342 and CO in both galaxies.

INTRODUCTION

We used the IRAM interferometer at Plateau de Bure (IRAM-PdB) (Guilloteau et al. 1992) to image the distribution of HCO^+ (J=1-0) and HCN (J=1-0) emissions in the inner 1' region of IC 342 and Maffei2 respectively. The synthesized beams were 2.4"x3.1" for IC 342 and 2.9"x3.5" for Maffei2. Since HCO^+ and HCN require higher densities than CO by at least two orders of magnitude to be collisionally excited, these observations trace the regions of dense gas in galactic nuclei.

IC342

We compared the distribution of the HCO^+ emission in the nuclear region of IC 342 with the distribution of the HCN emission obtained with the IRAM-PdB by Downes et al. (1992) and of the CO (J=1-0) emission obtained with the NMA by Ishizuki et al. (1990). For this purpose all the 3 data sets, at approximately the same angular resolution, were brought to a common 3D grid. We observe three main HCO^+ components which correspond very closely to the A, B and C (nomenclature of Downes et al.) HCN components. The HCN components D on the North and E on the South may have also HCO^+ counterparts. It has been argued that the HCO^+/HCN line ratio may reflect the nuclear activity (Nguyen-Rieu et al. 1992). The HCO^+ emission may be enhanced in regions rich in cosmic rays from supernova explosions. Since we found that the HCO^+ and HCN emissions are coextensive, the luminosities integrated over the solid angles and the line profiles of each cloud were measured inside the same volumes in the HCO^+ and HCN data cubes. These volumes were delineated by adding the HCO^+ cube with the HCN cube to increase the signal to noise ratio. The HCO^+ and HCN clouds are located in the very inner bar detected in CO (see Fig. 1). However, the strongest CO peak is not coincident with any HCO^+ or HCN peaks. The CO maximum intensity is shifted from the HCO^+-HCN peak of component C by ~3". The CO emission appears to be less clumpy than the HCO^+ and HCN emission, an expected result since CO traces more diffuse gas. The HCO^+/CO ratio was measured integrating in the CO data cube the emission over these same volumes. The cloud parameters are given in Tab. 1. The HCO^+/HCN ratio, ~0.85 ± 0.1, does not vary from cloud to cloud. There is a trend for the HCO^+/HCN ratio in clouds A and B to decrease radially outwards, from 1 to ~0.6, suggesting that HCO^+ is more confined towards the cloud centre. Unlike the HCO^+/HCN ratio, the HCO^+/CO ratio varies from cloud to cloud. Beside the fact that CO is less clumpy than HCO^+ and HCN, some CO complexes have no HCO^+ and HCN counterparts suggesting that they trace different regions. If the distance of IC342 is 1.8Mpc, the sizes of the individual clouds are ~35pc. This value is in the range of the sizes of the Giant Molecular Clouds in the centre of our Galaxy. The distribution of the continuum emission at 3mm has also been obtained by using the visibilities measured in the continuum during the HCO^+ and HCN observing sessions. We clearly distinguish three continuum sources, two of which almost coincident with clouds A and B have fluxes densities of respectively 4.0 ± 0.4 and 9.2 ± 0.5 mJy.

TABLE 1 Parameters of the clouds in IC 342

Cloud	RA	Dec	<V>	$\Delta V_{1/2}$	HCO^+	HCO^+/HCN	HCO^+/CO	size
	(1950)		(km/s)		(Jy km/s)			(arcsec)
A	3:41:53.7	67:56:25	23.5±2.0	13.5±3.0	7.2±1.0	0.85±0.05	0.072±0.01	2.8
B	3:41:56.8	67:56:26	25.2±2.0	13.1±3.0	6.2±1.0	0.78±0.05	0.068±0.01	4.0
C	3:41:58.0	67:56:31	49.5±1.0	23.5±2.0	7.6±1.0	0.93±0.1	0.054±0.01	3.9
D	3:41:57.9	67:56:38	~52	~19	~5	-	-	-
E	3:41:56.5	67:56:24	18.3±2.0	~6	3.8±1.0	0.93	0.038	2.0

MAFFEI2

Two fields were observed with the IRAM-PdB to image the distribution of HCN emission in Maffei2. Three HCN cloud complexes are clearly seen in the map of integrated HCN emission (Fig. 2). The most important complex (A) in the north direction, which has a very broad profile (115km/s FWHM), consists of at least 2 or 3 cloud components at -107, -67 and possibly -55 km/s with peak intensities of 0.17, 0.19 and 0.10 Jy/beam respectively. Complex B, which is ~10" south of complex A also contains more than one individual cloud. This complex B is probably associated with the nucleus of Maffei2 since its position is shifted (towards the east) from that of the nucleus by only ~2". The HCN properties of these complexes are listed in Tab. 2.

TABLE 2 HCN parameters of cloud complexes in Maffei2.

Cloud	RA	Dec	<V>	$\Delta V_{1/2}$	HCN	size	Remark
	(1950)		(km/s)		(Jy km/s)	(arcsec)	
A	2:38:08.4	59:23:33	-75±1	115	17±1	confused	2 to 3 components
B	2:38:08.2	59:23:22	-11±1	50	6.5±1	4	

The distribution of the continuum emission at 3.4 mm was also imaged with the IRAM-PdB. The strongest emission peak do not coincide with the nuclear Hα peak; it is rather near complex A north of the nucleus. The large scale distributions of the HCN and the 3mm continuum are similar to that of the Hα emission, most of these emissions being located on and North of the nucleus. In contrast, the CO observed by Ishiguro et al. (1989) is almost symmetric about the nucleus.

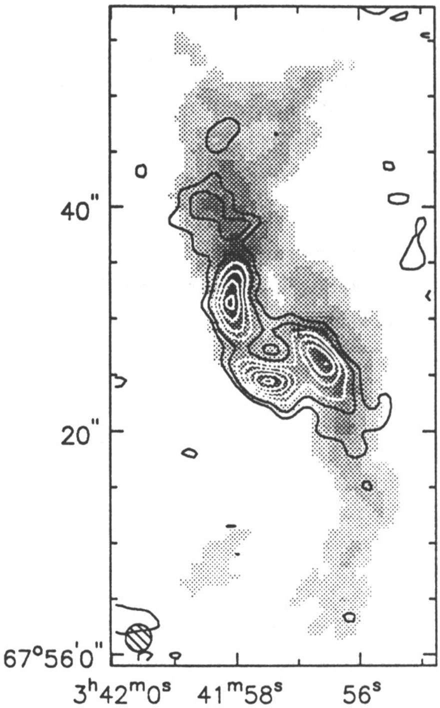

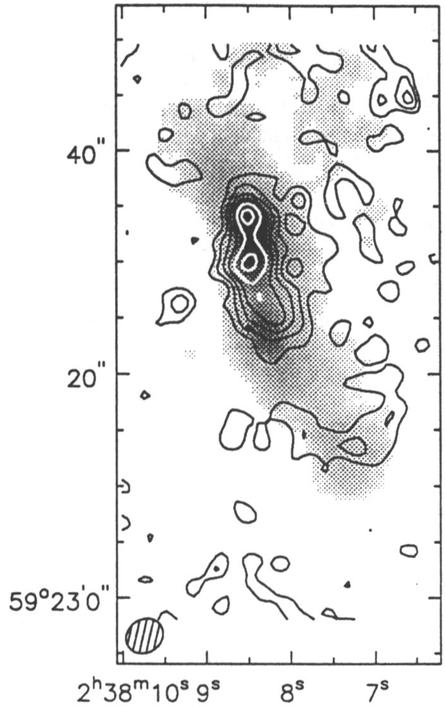

Fig. 1 (left): Distribution of the total HCO^+ line in IC342 (contour interval and first contour 0.5 Jy km s^{-1} $beam^{-1}$) superposed on the distribution of the total CO emission (grayscale). Fig. 2 (right): Radio continuum emission at λ3mm in Maffei2 (contour interval and first contour 0.5 mJy $beam^{-1}$) superposed on the distribution of total HCN emission (grayscale).

REFERENCES

Downes, D., Radford, S., Guilloteau, S., Guélin, M., Greve, A., Morris, D. 1992 A&A 262, 424

Guilloteau S., Delannoy, J., Downes, D., Greve, A., Guélin, M., Lucas, R., Morris, D., Radford, S., Wink, J., Cernicharo, J., Forveille, T., Garcia-Burillo, S., Neri, N., Blondel, J., Perrigouard, A., Plathner, D., Torres, M. 1992 A&A 262, 624

Ishiguro, M., Kawabe, R., Morita, K.-I., Okumura, S.K., Chikada, Y., Kasuga, T., Kansawa, T., Iwashita, H., Handa, K., Takahashi, T., Kobayashi, H., Murata, Y., Ishizuki, S., Nakai, N. 1989 ApJ 344, 763

Ishizuki, S., Kawabe, R., Ishiguro, M., Okumura, S.K., Morita, K.-I., Chikada, Y., Kasuka, T. 1990 Nature, 344, 224

Nguyen-Rieu et al. 1992 ApJ 399 Nov 10 Issue

https://doi.org/10.1017/S0252921100019886 Published online by Cambridge University Press